Laser heating in diamond anvil cells: developments in pulsed and continuous techniques

Alexander F. Goncharov,* Javier A. Montoya, Natarajan Subramanian, Viktor V. Struzhkin, Anton Kolesnikov, Maddury Somayazulu and Russell J. Hemley

Geophysical Laboratory, Carnegie Institution of Washington, Washington, DC 20015, USA.
E-mail: goncharov@gl.ciw.edu

Developments in continuous and pulsed laser-heating techniques, and finite-element calculations for diamond anvil cell experiments are reported. The methods involve the use of time-resolved (5 ns gated) incandescent light temperature measurements to determine the time dependence of heat fluxes, while near-IR incandescent light temperature measurements allow temperature measurements to as low as 500 K. Further optimization of timing in pulsed laser heating together with sample engineering will provide additional improvements in data collection in very high P–T experiments.

1. Introduction

Laser-heating diamond anvil cell (LHDAC) techniques represent a fast developing tool for the study of materials under extreme conditions of high pressures and temperatures. With these methods, investigations are now possible at pressures and temperatures approaching the center of the Earth. As such, these experimental studies are having a profound impact on fields that include Earth science, planetary science and new materials chemistry. Examples of ground-breaking results include synthesis of postperovskite (Murakami *et al.*, 2004), novel 'noble' metal nitrides (Gregoryanz *et al.*, 2004) and monatomic nitrogen (Eremets *et al.*, 2004), melting of iron

(Boehler, 1993), spin crossover and transport properties of iron-bearing minerals (Lin *et al.*, 2007; Ohta *et al.*, 2008), melting lines and molecular dissociation of simple molecular solids, H_2 (Gregoryanz *et al.*, 2003; Goncharov & Crowhurst, 2006; Deemyad & Silvera, 2008), H_2O (Goncharov *et al.*, 2005; Lin *et al.*, 2005) and N_2 (Mukherjee & Boehler, 2007; Goncharov *et al.*, 2008*a*). LHDAC methods can now be combined with a variety of experimental techniques including synchrotron X-ray diffraction (Dubrovinsky *et al.*, 2007) and X-ray spectroscopy (Lin *et al.*, 2005), optical spectroscopy (Lin *et al.*, 2004; Goncharov & Crowhurst, 2005) and visual observations [*e.g.* using laser speckle methods (Boehler, 2000)]. In view of the new outstanding opportunities which this technique offers, it may be rewarding to consider its further improvements. Here, we present an overview of recent developments in laser-heating techniques, which include a pulsed and a double-side continuous wave (CW) laser heating combined with Raman spectroscopy.

2. Results and discussion

2.1. Pulsed laser heating

Pulsed laser heating was proposed approximately 25 years ago (Gold *et al.*, 1984) and has recently advanced to a new level (Rekhi *et al.*, 2003; Deemyad *et al.*, 2005; Funamori & Sato, 2006; Beck *et al.*, 2007; Goncharov *et al.*, 2008*a,b*). Apart from reaching substantially higher temperatures than does continuous heating (>12000 K as currently reached and measured, Fig. 1), this technique also holds the promise of overcoming problems of containing and probing chemically reactive and mobile materials [*e.g.* H_2 (Deemyad & Silvera, 2008)]. Our approach includes the use of *in situ* time-resolved

Figure 1
Example of the incandescent spectrum measured in the DAC at 124 GPa with 10 ns temporal resolution. The uncertainty in temperature determination is given at the 1σ level.

Table 1
Thermochemical parameters of materials used in FE calculations.

	Diamond	Medium	Coupler
Density (kg m^{-3})	3500	5400	22650
Thermal conductivity (W m^{-1} K^{-1}) (300 K)	2000	50	300
Specific heat capacity (J kg^{-1} K^{-1})	509	1640	130

techniques for spectra-radiometric temperature and Raman/ optical spectroscopy measurements in pulsed laser-heated DACs (Beck *et al.*, 2007; Goncharov *et al.*, 2008*a*,*b*). These methods are complemented by finite-element calculations, which provide an important insight into the temporal temperature distributions across the sample cavity.

2.2. Finite-element calculations in DACs

Finite-element (FE) calculations have been performed using a commercial FlexPDE6 three-dimensional professional code. A special script has been developed for DACs calculations (Montoya *et al.*, 2010). Fig. 2 compares temperature profiles calculated for a continuous and pulsed (8 ns pulse width) double-side laser-heated cavity of DACs with dimensions and thermochemical parameters of materials approximately corresponding to 50 GPa. The values of the parameters used (Table 1) are not meant to be very accurate, since the calculations are only intended for illustrative purpose and for qualitative comparison between CW and pulsed heating. A sufficient portion of diamond anvils were included in the simulation domain; the results were found to be essentially
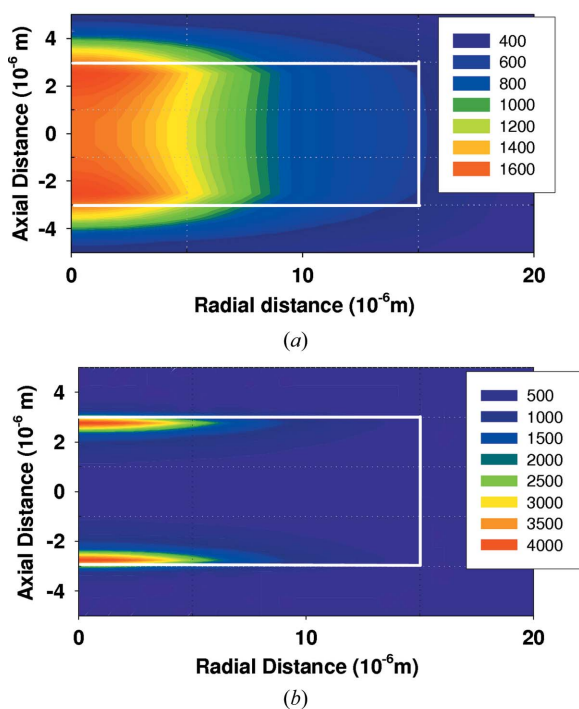
Figure 2
Finite-element calculations of the temperature profiles in the DAC cavity. (*a*) Continuous heating. (*b*) Pulsed heating.
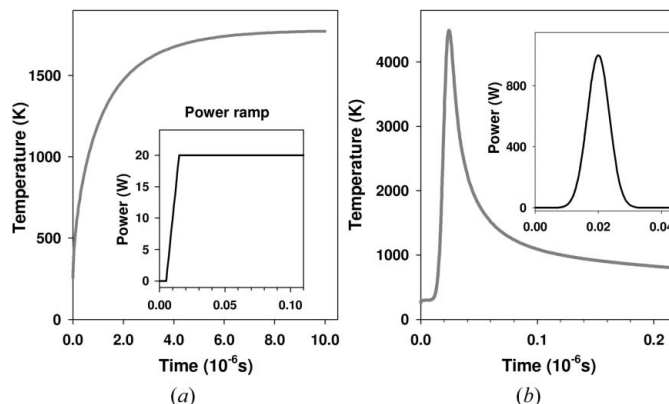
Figure 3
Finite-element calculations of the coupler surface temperature in the center of a laser-heating spot. (*a*) Continuous heating after turning on power. (*b*) Pulsed heating.

independent of their thickness [50 µm-thick diamonds were included in the final calculations, see Kiefer & Duffy (2005)]. A metal disc of thickness 6 µm was positioned in the geometrical center of the cavity (filled with a pressure-transmitting medium serving also as thermal insulation) to absorb the laser radiation (coupler). The temperature dependence of the thermal conductivity was incorporated into calculations in a manner similar to that reported in previous FE calculations (Kiefer & Duffy, 2005). The laser beam spot was assumed to have a Gaussian intensity profile at the focal spot with diameter 15 µm (full width at 1/*e*). In the case of pulsed laser heating, the temperature profile approximately corresponds to the moment when the maximum of temperature is reached at the coupler–medium interface. The temperature profile for continuous laser heating corresponds to the steady state, which is reached approximately 10 µs after the laser is turned on (Fig. 3). One can see that temperature profiles are much sharper in the case of pulsed laser heating, thereby allowing much higher temperatures to be reached than in the continuous case. On the other hand, the amount of material that is being heated is in the submicrometer range, which makes probe diagnostics very challenging. To make use of advantages of pulsed heating such as lower averaged power and the resulting reduced chemical reactivity, one can use longer pulses (µs range) and perform measurements at the time delayed window (tens of µs range) when the temperature profiles become less sharp and approach those for the continuous laser heating (Goncharov *et al.*, 2008*a*).

2.3. Continuous laser heating

We have recently upgraded our CW laser-heating Raman system (Lin *et al.*, 2004; Goncharov *et al.*, 2005; Goncharov & Crowhurst, 2006) to include a double-sided heating option, to use an ytterbium fiber laser, to provide a flat-top laser-heating spot (Prakapenka *et al.*, 2008), and to measure spectra-radiometric temperature in the near-IR spectral range (*e.g.* Deemyad & Silvera, 2008). We have also recently installed a single-frequency solid-state 458 nm laser as a Raman excitation source in addition to an Ar ion laser that provides lines
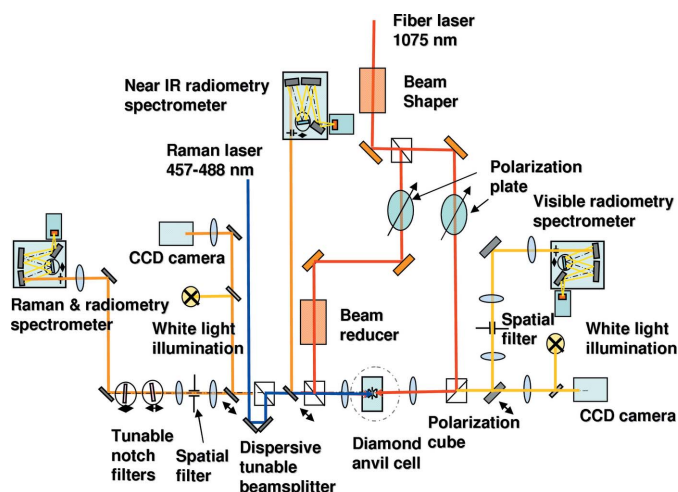
Figure 4
Optical layout of our combined Raman and continuous-wave laser-heating system.

Figure 5
Experimentally determined intensity profile of a laser-heating spot in a focal plane of a laser-heating system with a π-Shaper®.

Figure 6
Example of the incandescent spectrum measured in a laser-heated DAC using a InGaAs nitrogen-cooled array detector. The uncertainty in temperature determination is given at the 1σ level.

in the 458–514.5 nm spectral range. We are in the process of further upgrading the system by implementing an automatic control over the laser power and Raman/radiometric spectra measurements. All these modifications are aimed at making the operation more robust. A schematic of the system is shown in Fig. 4.

Similar to the optical arrangement described by Goncharov *et al.* (2005) and Goncharov & Crowhurst (2006), an un-polarized output beam of the fiber laser is split into two beams with orthogonal polarizations using a polarizing beam-splitter cube. Two other polarizing beam-splitter cubes are used to inject these two heating laser radiation beams into the Raman/radiometry system from both the sample sides. These polarizing cubes reflect virtually 100% of the p-polarized IR laser radiation (1075 nm) and transmit very well in the visible spectral range (*e.g.* there are no ripples characteristic of dichroic beam-splitters). The laser-heating power can be controlled independently at each sample side by rotating a $\lambda/2$ waveplate (which rotates the polarization plane). The net laser output power can also be controlled by changing the laser diode current; this does not change the mode state and quality. Mitutoyo near-IR 20× and 10× long-working distance objective lenses are employed for sample visualization, focusing the fiber laser in the sample, collection of radiation spectra in the visible (all from both sides), and collection of Raman and near-IR radiation spectra (from one side) in the axial geometry. A separate beam expander (acting as a beam contractor) is used in combination with a 20× Mitutoyo lens to match the IR fiber laser beam diameter and the entrance pupil of the lens and also to move the position of the focused laser spot in depth with respect to the focal plane of the lens. A π-Shaper® was positioned in the fiber laser beam approximately 1000 mm upstream of the lens to provide a flat-top beam intensity profile of approximately 12 µm diameter (35 µm at $1/e^2$) in the focal plane of the 20× lens (Fig. 5).

For radiometric temperature measurements in the near-IR range we set up a dedicated system that consists of a 300 mm focal length spectrograph equipped with 150 groove mm^{-1} grating and an InGaAs nitrogen-cooled array detector. The spectra were recorded at 1400–1600 nm; the typical accumulation time was 0.1 s. The spectral output was calibrated with a standard tungsten coiled-coil filaments lamp (Optronic Laboratories). Using this system, we were able to measure temperatures as low as 500 K (Fig. 6). A background signal (of presumably fluorescent origin) presents a problem for such low T measurements in the case of laser heating. It can be at least partly remedied by choosing narrower spectral (further from the excitation, *e.g.* >1400 nm) and by careful background subtraction.
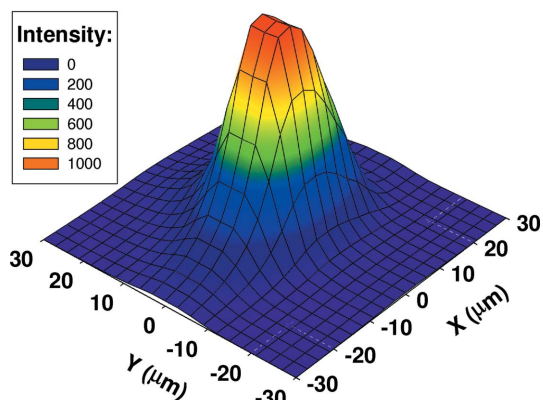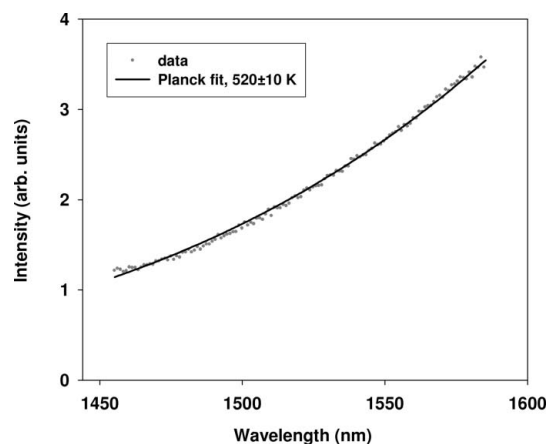
3. Conclusions

Pulsed laser techniques allow higher temperature to be reached routinely but in much smaller volumes compared with CW heating. Time-resolved measurements of temperature by radiometry are feasible and represent an important diagnostic of time-dependent heat fluxes in the DACs. Radiometric measurements in the near-IR using an InGaAs array detector allow temperature determination as low as 500 K.

Time-dependent FE calculations in the DACs, which we have developed, are an essential tool for planning laser-heating experiments and interpreting their results. They provide better understanding and quantitative results on the spatial temperature profiles and their time dependence. Time-domain laser-heating techniques combined with FE calculations open new opportunities for DACs experiments [*e.g.* measurements of the thermal diffusivity, see Beck *et al.* (2007)].

References

Beck, P., Goncharov, A. F., Struzhkin, V. V., Militzer, B., Mao, H.-K. & Hemley, R. J. (2007). *Appl. Phys. Lett.* **91**, 181914.

Boehler, R. (1993). *Nature (London)*, **363**, 534–536.

Boehler, R. (2000). *Rev. Geophys.* **38**, 221–245.

Deemyad, S. & Silvera, I. F. (2008). *Phys. Rev. Lett.* **100**, 155701.

Deemyad, S., Sterer, E., Barthel, C., Rekhi, S., Tempere, J. & Silvera, I. F. (2005). *Rev. Sci. Instrum.* **76**, 125104.

Dubrovinsky, L., Dubrovinskaia, N., Narygina, O., Kantor, I., Kuznetzov, A., Prakapenka, V. B., Vitos, L., Johansson, B., Mikhaylushkin, A. S., Simak, S. I. & Abrikosov, I. A. (2007). *Science*, **316**, 1880–1883.

Eremets, M. I., Gavriliuk, A. G., Trojan, I. A., Dzivenko, D. A. & Boehler, R. (2004). *Nat. Mater.* **3**, 558–563.

Funamori, N. & Sato, T. (2006). *Rev. Sci. Instrum.* **77**, 093903.

Gold, J. S., Bassett, W. A., Weathers, M. S. & Bird, J. M. (1984). *Science*, **225**, 921–922.

Goncharov, A. F., Beck, P., Struzhkin, V. V., Hemley, R. J. & Crowhurst, J. C. (2008*b*). *J. Phys. Chem. Solids*, **69**, 2217–2222.

Goncharov, A. F. & Crowhurst, J. C. (2005). *J. Low Temp. Phys.* **139**, 727–737.

Goncharov, A. F. & Crowhurst, J. C. (2006). *Phys. Rev. Lett.* **96**, 055504.

Goncharov, A. F., Crowhurst, J. C., Struzhkin, V. V. & Hemley, R. J. (2008*a*). *Phys. Rev. Lett.* **101**, 095502.

Goncharov, A. F., Goldman, N., Fried, L. E., Crowhurst, J. C., Kuo, I. F. W., Mundy, C. J. & Zaug, J. M. (2005). *Phys. Rev. Lett.* **94**, 125508.

Gregoryanz, E., Goncharov, A. F., Matsuishi, K., Mao, H. K. & Hemley, R. J. (2003). *Phys. Rev. Lett.* **90**, 175701.

Gregoryanz, E., Sanloup, C., Somayazulu, M., Badro, J., Fiquet, G., Hemley, R. J. & Mao, H. K. (2004). *Nat. Mater.* **3**, 294–297.

Kiefer, B. & Duffy, T. S. (2005). *J. Appl. Phys.* **97**, 114902.

Lin, J. F., Gregoryanz, E., Struzhkin, V. V., Somayazulu, M., Mao, H. K. & Hemley, R. J. (2005). *Geophys. Res. Lett.* **32**, L11306.

Lin, J. F., Santoro, M., Struzhkin, V. V., Mao, H. K. & Hemley, R. J. (2004). *Rev. Sci. Instrum.* **75**, 3302–3306.

Lin, J. F., Vankó, G., Jacobsen, S. D., Iota, V., Struzhkin, V. V., Prakapenka, V. B., Kuznetsov, A. & Yoo, C. S. (2007). *Science*, **317**, 1740–1743.

Montoya, J. A. *et al.* (2010). In preparation.

Mukherjee, G. & Boehler, R. (2007). *Phys. Rev. Lett.* **99**, 225701.

Murakami, M., Hirose, K., Kawamura, K., Sata, N. & Ohishi, Y. (2004). *Science*, **304**, 855–858.

Ohta, K., Onoda, S., Hirose, K., Sinmyo, R., Shimizu, K., Sata, N., Ohishi, Y. & Yasuhara, A. (2008). *Science*, **320**, 89–91.

Prakapenka, V. B., Kubo, A., Kuznetsov, A., Laskin, A., Shkurikhin, O., Dera, P., Rivers, M. L. & Sutton, S. R. (2008). *High Press. Res.* **28**, 225–235.

Rekhi, S., Tempere, J. & Silvera, I. F. (2003). *Rev. Sci. Instrum.* **74**, 3820–3825.